(12)

DAVID W. TAYLOR NAVAL SHIP RESEARCH AND DEVELOPMENT CENTER

Bethesda, Md. 20084

ELEMENTS OF THE DRAG OF UNDERWATER BODIES

by

Paul S. Granville

APPROVED FOR PUBLIC RELEASE: DISTRIBUTION UNLIMITED

SHIP PERFORMANCE DEPARTMENT
DEPARTMENTAL REPORT

June 1976 SPD-672-01

MAJOR DTNSRDC ORGANIZATIONAL COMPONENTS

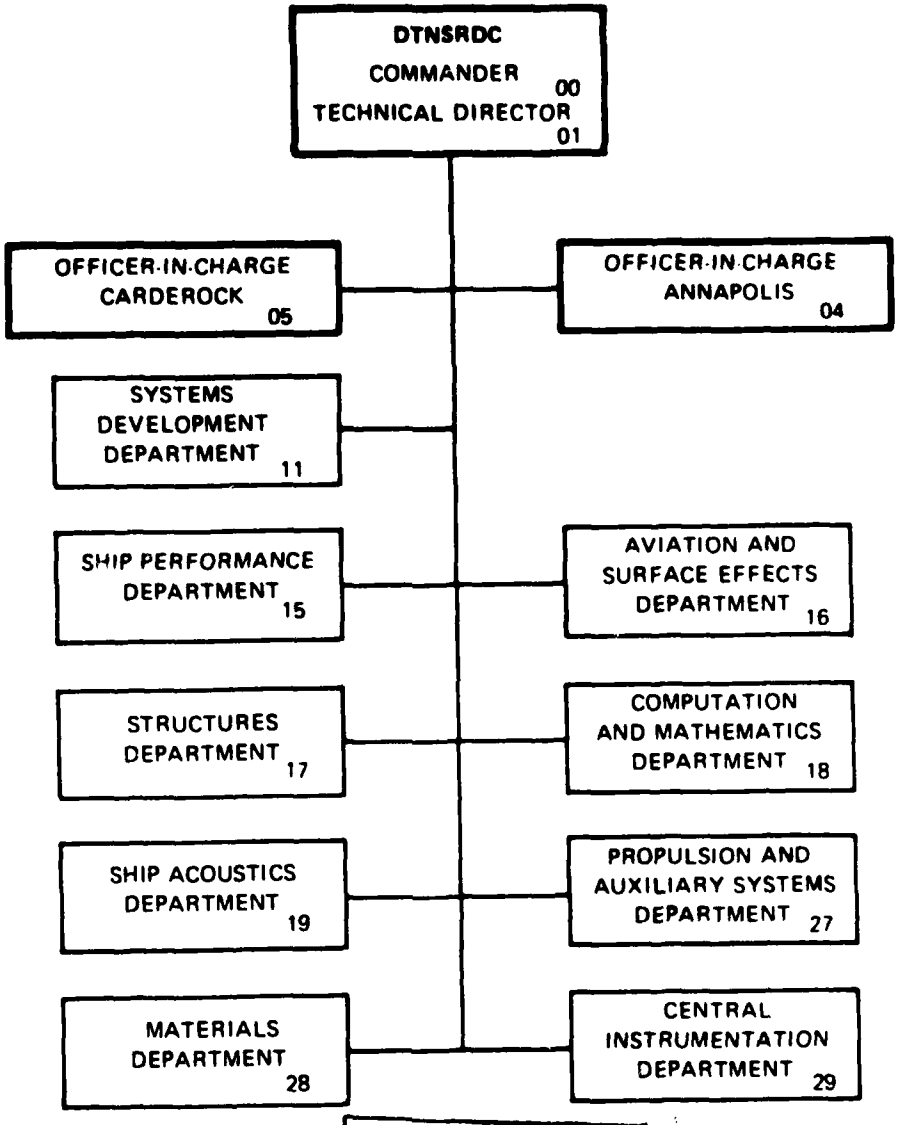

UNCLASSIFIED

SECURITY CLASSIFICATION OF THIS PAGE (When Data Entered)

REPORT DOCUMENTATION PAGE		READ INSTRUCTIONS BEFORE COMPLETING FORM
1. REPORT NUMBER (14) SPD-672-01	2. GOVT ACCESSION NO.	3. RECIPIENT'S CATALOG NUMBER
4. TITLE (and Subtitle) (6) Elements of the Drag of Underwater Bodies.		5. TYPE OF REPORT & PERIOD COVERED (9) Final rept.,
		6. PERFORMING ORG. REPORT NUMBER
7. AUTHOR(s) (10) Paul S. Granville		8. CONTRACT OR GRANT NUMBER(s)
9. PERFORMING ORGANIZATION NAME AND ADDRESS David Taylor Naval Ship R&D Center Bethesda, Md. 20084 Ship Perf. Dept		10. PROGRAM ELEMENT, PROJECT, TASK AREA & WORK UNIT NUMBERS 61151N NR 12301-03
11. CONTROLLING OFFICE NAME AND ADDRESS Naval Sea Systems Command Washington, DC 20360		12. REPORT DATE (11) June 1976
		13. NUMBER OF PAGES (12) 33p.
14. MONITORING AGENCY NAME & ADDRESS(if different from Controlling Office)		15. SECURITY CLASS. (of this report) UNCLASSIFIED
		15a. DECLASSIFICATION/DOWNGRADING SCHEDULE

16. DISTRIBUTION STATEMENT (of this Report)

Approved for public release; distribution unlimited

17. DISTRIBUTION STATEMENT (of the abstract entered in Block 20, if different from Report)

18. SUPPLEMENTARY NOTES

19. KEY WORDS (Continue on reverse side if necessary and identify by block number)

drag, underwater bodies, drag reduction

20. ABSTRACT (Continue on reverse side if necessary and identify by block number)

Elementary aspects of the drag of underwater bodies are reviewed. Shape and boundary-layer concepts are included. Optimization of shape is considered and drag reduction is discussed.

DD FORM 1 JAN 73 1473 EDITION OF 1 NOV 65 IS OBSOLETE S/N 0102-014-6601 |

UNCLASSIFIED

SECURITY CLASSIFICATION OF THIS PAGE (When Data Entered)

389694

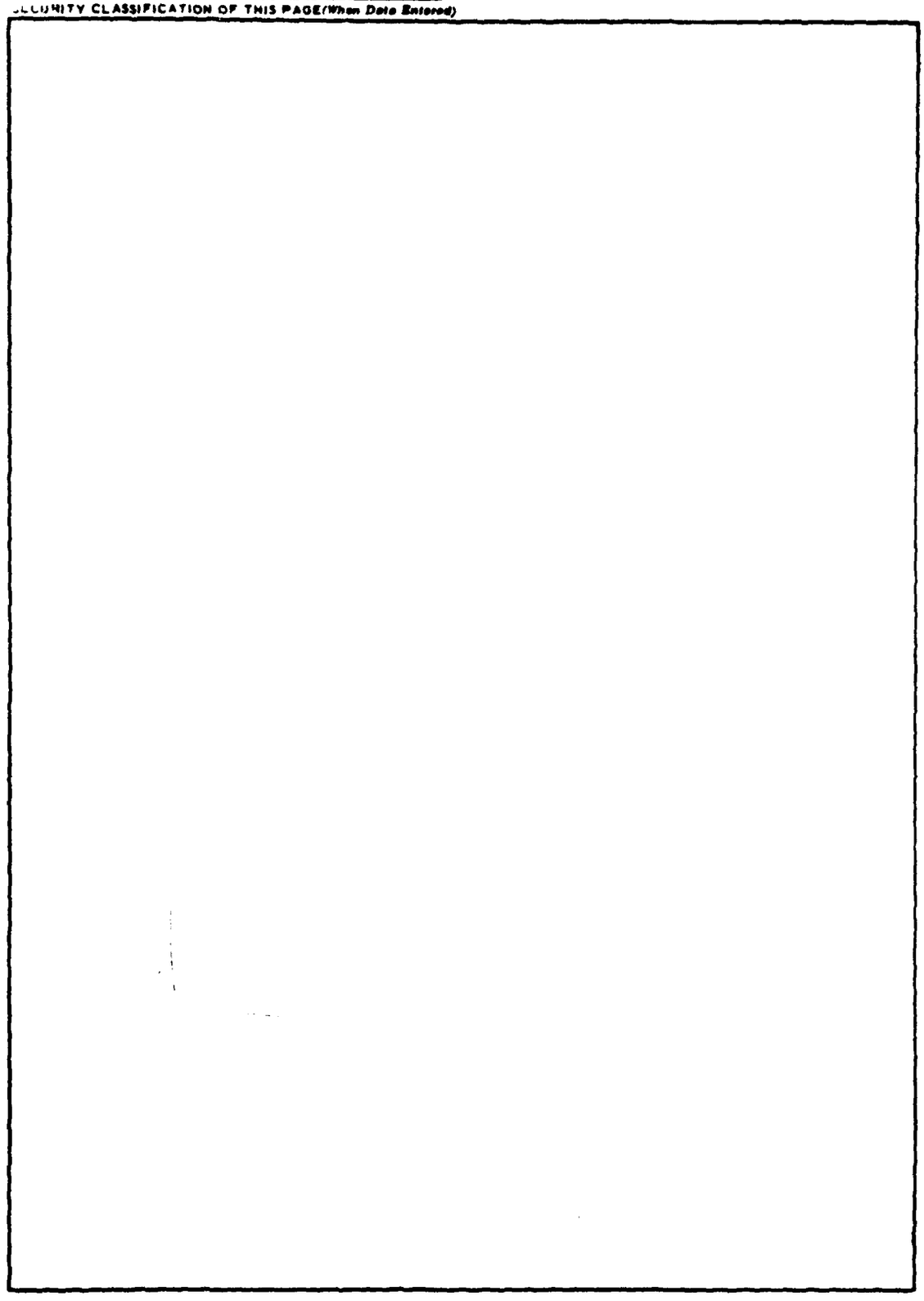

NOTATION

C_a	Appendage drag coefficient
C_D	Drag coefficient based on surface area, Equation (12)
$\textcircled{C_D}$	Drag coefficient based on volume, Equation (23)
$C_{D,b}$	Drag coefficient of bare body
C_F	Drag coefficient of flat plates
C_p	Pressure coefficient
C_r	Form or residual drag coefficient
C_s	Surface-area coefficient
C_v	Volume (prismatic) coefficient
D_a	Appendage drag
D	Drag
e	Subscript referring to end of body of revolution
k_a	Appendage drag factor
k	Form factor
L	Length of body
$L_1, L_2, \ldots$	Length parameters
m	Exponent
n	Exponent
p	Pressure
p_∞	Static pressure at centerline of body
R	Maximum radius of body
R_L	Reynolds number, $R_L = U_\infty L/\nu$
r	Radius of body
S	Surface area of body

S_a	Appendage surface area
U	Velocity at outer edge of boundary layer
U_∞	Forward velocity
V	Volume of body
x	Axial distance from nose
α	Angle of tangent to body contour
ν	Kinematic viscosity of water
ρ	Density of water

DRAG OF UNDERWATER BODIES

General Aspects of Drag

In the absence of a free surface, a body moving in water or any other fluid at constant speed experiences a resisting force opposing its motion along its line of direction which may be termed viscous drag or viscous resistance. On the other hand, an inviscid fluid would result in no drag for steady motion (D'Alembert's paradox). However, it is to be noted that an inviscid fluid does provide resistance to accelerated motion.

Viscous drag may also be considered the resultant force along the line of motion of hydrodynamic stresses acting on the body surface which may be resolved into a normal stress or pressure and a tangential stress or skin friction. The relative magnitudes of the pressure contribution and of the skin friction contribution to drag vary depending on the body shape. A streamlined body, that is one with negligible separation on its stern, has primarily skin-friction drag. A principal aim of good body design is to minimize pressure drag since values of pressure drag may reach magnitudes much greater than those for skin-friction drag.

Viscous drag is intimately connected with the boundary-layer development on the body. Any detailed analysis of viscous drag requires a detailed analysis of the associated boundary layer.

Geometry

Shape and size are the two principal geometric parameters controlling the drag of underwater bodies as well as other hydrodynamic characteristics such as cavitation. Shape and size determine the relative values of the surface area and of the pressure distribution which influences the drag of the outer shell enclosing the required volume of propulsion machinery and payload.

Size is given by specifying the overall dimensions of a body: two for a two-dimensional body and three for a three-dimensional body. A body of revolution is basically a quasi two-dimensional body since its size is given by its overall length and maximum diameter.

Shape

Shape may be defined as the relative proportions of a body's contour which may be expressed analytically in terms of a function description of the body surface. For bodies of revolution with radius r as a function of axial distance x from the nose, the shape is given by the function f

$$\frac{r}{R} = f\left[\frac{x}{L}\right] \tag{1}$$

where R is the maximum radius and L the length of the body. Shapes of different bodies may be classified on the basis of geometrical similarity.

Simple Geometric Similarity

The class of bodies of revolution with simple geometric similarity is given by

$$\frac{r}{R} = f\left[\frac{x}{L}, \frac{R}{L}\right] \tag{2}$$

where R/L is constant. Bodies with simple geometric similarity are considered to have the same shape. Spheres of any size are bodies of revolution which have inherent simple geometric similarity and hence have the same shape.

Stretched or Affine Geometric Similarity

Keeping the same basic geometry but stretching or contracting the length relative to the maximum radius that is, $R/L \neq$ const, provides a kind of similarity of shape. Analytically, for a body of revolution, equation (2) holds when the function f is kept the same but R/L is varied.

An example is the class of confocal ellipsoids where the ratio of major to minor axes varies.

Systems Geometric Similarity

A looser type of shape similarity, which may be termed systems similarity, is given for the class of bodies where additional parameters are varied. This is illustrated further on.

Examples of Types of Similarity

Let us examine the class of bodies known as generalized ellipsoids analytically stated as

$$\left(\frac{r}{R}\right)^m + \left[\frac{x - (L/2)}{L/2}\right]^n = 1 \tag{3}$$

or

$$\frac{r}{R} = \left[1 - \left(\frac{2x}{R} \cdot \frac{R}{L} - 1\right)^n\right]^{\frac{1}{m}} \tag{4}$$

Ordinary ellipsoids are specified when $m,n = 2$.

Simple geometric similarity occurs when

m,n = const

R/L - const

$R \neq$ const

Stretched geometric similarity occurs when

m,n = const

R or L = const

$R/L \neq$ const

Systems geometric similarity occurs when

R,L = const

m and/or $n \neq$ const

As an example, the Reichardt body which provides an almost constant pressure distribution is a generalized ellipsoid with

$m = 2.4, n = 2$

Geometric Systems for Streamlined Shapes

Most underwater bodies of revolution are designed to be streamlined with a rounded or flat-faced nose, a tapering tail, and usually a cylinder in between. However, since simple geometric figures are often used such as an ellipsoidal nose or a paraboloid tail, discontinuities in curvature

result at the junctions with the cylindrical middle body. At high speeds, such curvature discontinuities may give rise to vortex production, earlier inception of cavitation, and increases in drag. Hence, curvature discontinuities should be avoided in the design of bodies.

Classes of bodies suitable for streamlined shapes are given in References* 1, 2, and 3 in terms of polynomials controlled by geometric parameters. Rounded and flat-faced noses and various tail configurations may be found in these references. All the shapes are designed to avoid any discontinuities in curvature at junctions.

Geometrical Factors

In designing streamlined underwater bodies, surface area is of prime importance in determining drag and enclosed volume is important in determining the usefulness of the vehicle. For a body of revolution, surface area S is given by

$$S = 2\pi \int_0^L r \sqrt{1 + \left(\frac{dr}{dx}\right)^2} \, dx \tag{5}$$

and volume V by

$$V = \pi \int_0^L r^2 \, dx \tag{6}$$

Surface Area Coefficient

A coefficient useful for determining surface area from overall dimensions is C_s, the surface area coefficient which is defined by the ratio of the surface area to that of the circumscribing cylinder or

$$C_S = \frac{S}{2\pi RL} \tag{7}$$

Then

$$S = C_S \, 2\pi RL \tag{8}$$

C_s is a constant for bodies with simple geometric similarity. For prolate

* References are found on page 16.

ellipsoids and cones C_s increases slowly with diameter-length ratio as shown ir Figure 1. For cylinders $C_s = 1$.

igure 1 also shows the values of C_s for the Mark 41 torpedoes with varying lengths of parallel middle body; the surface area of the control surfaces is included in the overall surface area.

Volume Coefficient

Another coefficient, useful for determining the volume of the body from overall dimensions, is C_v, the volume coefficient (the prismatic coefficient in the parlance of naval architecture) which is defined as the ratio of the volume to that of the circumscribing cylinder or

$$C_V = \frac{V}{\pi R^2 L} \tag{9}$$

Then

$$V = C_V \pi R^2 L \tag{10}$$

C_v is a constant for bodies with simple and with distorted geometrical similarity. For all diameter-length ratios, $C_v = 2/3$ for prolate ellipsoids; $C_v = 1/3$ for cones and $C_v = 1$ for cylinders. Figure 1 also shows values of C_v for the Mark 41 torpedoes with varying lengths of parallel middle body.

Surface Area to Volume Ratio

The ratio of S to V is given by

$$\frac{S}{V} = \left(\frac{C_s}{C_v}\right) \left(\frac{2}{R}\right) \tag{11}$$

For bodies with simple geometric similarity, C_s and C_v are constant and hence $\frac{S}{V}$ varies inversely with R; that is, the larger the body, the smaller the surface area relative to volume and consequently the less relative drag.

Drag Coefficient

The drag D of a body may be stated in terms of a drag coefficient C_D

$$C_D = \frac{D}{(1/2)\rho U_\infty^2 S} \tag{12}$$

where ρ is the density of the water, U_∞ is the forward velocity, and S is the wetted surface area.

In the fully-submerged condition away from the free surface, C_D is a function of Reynolds number R_L and body shape given by length ratios L/L_1, L/L_2, L/L_3,... or

$$C_D = f\left[R_L, L/L_1, L/L_2, L/L_3, \ldots\right] \tag{13}$$

where

$$R_L = \frac{U_\infty L}{\nu}$$

ν = kinematic viscosity of water

L_1, L_2, L_3,..... = additional length parameters defining the body

For a body of revolution usually $L_1 = 2R$, the maximum diameter. Also bodies with simple geometric similarity have a unique relationship between C_D and R_L.

Form Drag

A flat plate parallel to the flow represents a body with no form drag; the drag is entirely due to skin friction with no pressure drag present.

A body of revolution in axial motion has a varying pressure p over its surface which for deep submergences away from the free surface is solely a function of axial position. It may be expressed in terms of a pressure coefficient C_p defined by

$$C_p = \frac{P - P_\infty}{(1/2)\rho U_\infty^2} \tag{14}$$

where p_∞ = static pressure at centerline. At the stagnation point, $C_p = 1$.

Associated with p is a velocity U which for thin boundary layers is the velocity outside the boundary layer. From Bernoulli's theorem

$$\left(\frac{U}{U_\infty}\right)^2 = 1 - C_p \tag{15}$$

At the stagnation point U = 0.

It is the presence of a varying p or U which provides the prime ingredient for form drag arising from the development of the boundary layer.

C_p may be determined from a potential flow calculation.[4] At the tail there is a small decrease in C_p due to the thickened boundary layer which also suppresses the theoretical after stagnation point. Any flow separation such as due to a blunt end further modifies C_p.

A form or residual drag may be defined by subtracting the drag of a flat plate of equal surface area moving at Reynolds number R_L (more realistically it is cylinder of equal surface area and Reynolds number) from the total drag. Then, in general,

$$C_r = C_D - C_F \tag{16}$$

or

$$C_D = C_F + C_r$$

where C_r = form or residual drag coefficient nondimensionalized on total surface area,

C_F = drag coefficient of flap plate nondimensionalized on total surface area.

C_r is a catchall coefficient. If the body surface is rough, C_r includes the added drag due to roughness. For appended bodies C_r includes the added drag not accounted for by adding the appendage surface area to the body surface area.

Drag Coefficients of Flat Plates

A well-accepted formulation for the drag coefficient of flat plates is that of Schoenherr

$$\frac{1}{\sqrt{C_F}} = 4.13 \log_{10} (R_L C_F) \tag{18}$$

Unfortunately C_F is an implicit function of R_L which requires a table for convenient evaluation.

A recent explicit formula[5] derived from boundary-layer theory agrees with the Schoenherr formula at high Reynolds numbers but is more accurate at low Reynolds numbers, namely,

$$C_F = \frac{0.0776}{(\log_{10} R_L - 1.88)^2} + \frac{60}{R_L} \qquad (19)$$

By a coincidence this formula gives values close to the International Towing Tank formula,[5] ITTC-1957, used to extrapolate the drag of ship models to full-scale conditions.

The variations of density and kinematic viscosity of fresh and of sea water with temperature are given in tables in the appendix.

Representative Measured Values of Form-Drag Coefficient

Measured values of the form of residual drag of towed bodies (References 6 through 11) have been assembled in Figure 2 where the form-drag coefficient C_r is plotted against diameter-length ratio. In general, the form-drag coefficient usually increases with increasing diameter-length ratio.

All the Mark numbered torpedoes have parallel middle bodies which are fully stabilized by fins and/or shrouds and control surfaces and whose surface area has been added to the body surface area. The Series 58 bodies shown are bare bodies without appendages.

Note in Curve A that the effect of adding more parallel middle body (indicated by numbers in parenthesis) to the Mark 41 torpedo is to decrease C_r. In Curve C adding parallel middle body to a Series 58 body results in an increased C_r. The latter result may be explained as the effect of the increased thickness of bodunary layer over the tail which slightly increases the pressure drag. In the Mark 41 torpedo this small effect may be overwhelmed by the large appendage and roughness drags.

The lower C_r values for the RETORC torpedo are for a smooth wooden wind-tunnel model unlike the Mark 41 torpedo with its roughness due to manufacturing processes.

Curve A represents the behavior of average operational underwater bodies which may be used for the estimation of the form drag of similar bodies. Other empirical procedures are given in References 12 and 13.

Relative Merits of Body Shape and Size

The usual comparison for the efficiencies of body shapes with

respect to drag is on the basis of equal volume. The following non-dimensional analysis may be made. The surface area and volume ratios are in general given by

$$\frac{S}{L^2} = f\left[L/L_1,\ L/L_2,\ L/L_3, \ldots\right] \tag{20}$$

$$\frac{V}{L^3} = f\left[L/L_1,\ L/L_2,\ L/L_3, \ldots\right] \tag{21}$$

$$\frac{S}{V^{2/3}} = f\left[L/L_1,\ L/L_2,\ L/L_3, \ldots\right] \tag{22}$$

If a drag coefficient, C_D, nondimensionalized on (volume)$^{2/3}$ is defined, then Equation (13) may be modified to give

$$C_D = \frac{D}{\frac{1}{2}\rho U_\infty^2 V^{2/3}} = f\left[\frac{U_\infty V^{1/3}}{\nu}, \frac{L}{L_1}, \frac{L}{L_2}, \frac{L}{L_3}, \ldots\right] \tag{23}$$

Two cases involving one independent geometric ratio only are examined in Figure 3 for the data shown in Figure 2: the fully-appended Mark 41 flat-faced bodies with varying lengths of parallel middle body, curve A, and an affine group of Series 58 bodies with varying fineness ratios, curve B. Here it is assumed that in the drag prediction the form resistance coefficient C_r is solely a function of geometry. Thus

$$C_D = C_F\left[\frac{U_\infty L}{\nu}\right] + C_r\left[\frac{L}{2R}\right] \tag{24}$$

Then

$$C_D = \left(C_F\left[\left(\frac{U_\infty V^{1/3}}{\nu}\right)\left(\frac{L}{V^{1/3}}\right)\right] + C_r\left[\frac{L}{2R}\right]\right)\left(\frac{S}{V^{2/3}}\right) \tag{25}$$

$$\frac{L}{V^{1/3}} = \left[\pi C_V \left(\frac{R}{L}\right)^2\right]^{-\frac{1}{3}} \tag{26}$$

$$\frac{S}{V^{2/3}} = 2\pi^{1/3}\frac{C_S}{C_V^{2/3}}\left(\frac{L}{R}\right)^{\frac{1}{2}} \tag{27}$$

Figure 3 shows that a minimum drag coefficient exists which is a function of fineness ratio L/2R and Reynolds number $(U_\infty \forall^{1/3})/\nu$. The higher L/2R values for the minimum drag coefficient of the Mark 41 torpedo may be due to its being rougher and having appendages unlike the smooth bare Series 58 bodies. The variation of fineness ratio with Reynolds number for minimum drag based on volume is shown in Figure 4 for Series 58 bodies having fixed values of $C_V = 0.65$.

In some situations design considerations dictate that the diameter 2R be kept fixed. Then the drag coefficient (C_D) defined by Equation (23) may be considered to represent the drag efficiency relative to the volume, $D/\forall^{2/3}$, and

$$(C_D) = f\left[\frac{U_\infty 2R}{\nu}, \frac{L}{2R}, \frac{L}{L_2}, \cdots\right] \tag{28}$$

Then

$$(C_D) = \left(C_F\left[\left(\frac{U_\infty 2R}{\nu}\right)\left(\frac{L}{2R}\right)\right] + C_r\left[\frac{L}{2R}\right]\right)\left(\frac{S}{\forall^{2/3}}\right) \tag{29}$$

Values of (C_D) as a function of $(U_\infty 2R)/\nu$ are shown in Figure 3 for the Mark 41 bodies and the Series 58 bodies. It is to be noted that the minimum values of L/2R *remain on the same curve.* The minimum values are also shown in Figure 4 for the fineness ratio L/2R as a function of diameter Reynolds number $(U_\infty 2R)/\nu$.

Drag from Boundary-Layer Development

Viscous drag is intimately associated with the development of the boundary layer on a body. The boundary layer is the usually thin region of flow next to the body where viscous effects predominate. As shown in Figure 5, the boundary layer starts at the stagnation point on the nose and increases in thickness downstream. The flow in the boundary layer is initially laminar and undergoes transition to turbulent flow. The higher the Reynolds number, the earlier the transition and the smaller the length of the laminar boundary layer. Laminar flow is more desirable since it engenders a much smaller skin friction. For most existing torpedoes the flow is primarily turbulent. An analytical approach to determining drag from the boundary layer development is given in Reference 14.

For bare streamlined bodies of revolution without appendages and with completely turbulent boundary layer, a drag coefficient $C_{D,b}$ may be determined from a simplified boundary-layer analysis by[15]

$$C_{D,b} = (1+k)\, C_F \tag{30}$$

where

$$1+k = \left[\frac{\int_0^1 \left(\frac{r}{L}\right)^{1.168b} \left(\frac{U}{U_\infty}\right)^{3.404b} \sec\alpha \; d\left(\frac{x}{L}\right)}{\int_0^1 \left(\frac{r}{L}\right)^{1.168b} \sec\alpha \; d\left(\frac{x}{L}\right)} \right]^{0.8557} \left(\frac{U}{U_\infty}\right)_e^{0.05} \tag{31}$$

k = form factor,

α = profile angle of body shape

$\sin\alpha = \frac{dr}{dx}$

e = subscript referring to conditions at after end of the body of revolution.

$\frac{U}{U_\infty}$ is obtained from pressure coefficient C_p, Equation (15).

The appendage drag may be evaluated by an empirical formula,[6] which may be restated as

$$C_a = k_a\, C_{D,b} \tag{32}$$

where C_a, the appendage drag coefficient, is given by

$$C_a = \frac{D_a}{\frac{1}{2}\rho U_\infty^2 S_a} \tag{33}$$

where D_a = appendage drag,

S_a = total appendage area,

k_a = appendage drag factor.

A value of $k_a = 2.3$ has been given[6] for the control surfaces of submarines. A value of $k_a = 1.8$ for torpedoes has been deduced from an unpublished analysis. The large value of k_a is due to the low local

value of the Reynolds number of the flow around the appendages and interference drag arising from body-appendage interaction.

Frictional Drag Reduction

Streamlining bodies to eliminate the pressure drag due to flow separation on the tail leaves frictional drag as the remaining drag component to be reduced. Outside of the obvious smoothing of the body surface, the reduction of frictional drag is a difficult technical process which is more or less still in various experimental and developmental stages.

Methods of reducing frictional drag may be classified as follows:

A. Extension of the laminar boundary layer through stabilization
   1. by shaping the forward part of the body (laminar-flow bodies) to provide sufficient favorable pressure gradient
   2. by mild suction through the body surface
   3. by compliant walls
   4. by heating the body surface

B. Reduction of turbulent skin friction
   1. by smoothing
   2. by polymer additives
   3. by compliant walls

Extension of Laminar Boundary Layer

Since laminar skin friction is about one order of magnitude less in value than turbulent skin friction, maintaining laminar flow in the boundary layer has obvious benefits in reducing the frictional drag. Also, since transition to turbulent flow is a result of a destabilizing process, maintaining the stability of the boundary-layer flow is required to delay transition. Destabilizing disturbances such as due to body roughness and to free-stream turbulence have to be eliminated as much as possible. A critical factor is the Reynolds number of the flow situation. The higher the Reynolds number, the more difficult the maintainance of laminar flow.[5]

Laminar-Flow Bodies

Shaping a body to create a favorable pressure gradient is a simple method of stabilizing the laminar flow in the boundary layer. Proper selection of a favorable pressure gradient will produce boundary-layer velocity profiles which are inherently stable over a range of Reynolds numbers. The so-called laminar-flow bodies tend to have the maximum section as far aft as possible and to be relatively thick compared to the usual underwater bodies in order to have comparable volumes. Reference 16 describes the successful development of one such body while Reference 17 describes an optimization procedure to obtain a body of least drag for stated operational requirements. The design of optimum laminar-flow bodies requires an accurate prediction of the position of transition as well as an accurate prediction of turbulent flow separation. Shaping the forward part of the body to delay transition may result in premature turbulent separation and an increase of form drag on the tail. Hence, shaping the tail is also important. Methods of predicting transition accurately on bodies of revolution are still being developed.[18,19]

Suction

The laminar boundary layer may be made more stable by mild suction at the wall to impart a normal velocity inward towards the body surface. More stable velocity profiles result which resist transition to turbulent flow. Too much suction would thin the boundary layer and produce a higher local skin friction.

Two techniques have been under development: continuous suction through a porous surface[20] and discontinuous suction through narrow slots[21] in the body surface. Slots are less subject to clogging but have the disadvantage of producing disturbances at their entrance through the body. Suction slots for drag reduction have been highly developed for aircraft wings but have yet to become operational.

Compliant Walls

Efforts to stabilize the laminar boundary layer on a compliant surface have achieved no clear-cut results. There are various claims[22] to its efficacy but no general acceptance. It is difficult to design a compliant surface to absorb a wide spectrum of disturbing frequencies.

Wall Heating

Heating the wall of a water boundary layer produces more stable velocity profiles[23] which tend to delay transition. However, unless the heat is available as a discard, the resulting drag reduction may not compensate for the high loss of thermal energy.

Reduction of Turbulent Skin Friction

At high Reynolds numbers, the flow in the boundary layer is usually turbulent which implies relatively high values of skin friction. The reduction of turbulent skin friction involves then an interference of some kind in the turbulence mechanism producing the high shearing stresses at the wall. Since there is no satisfactory general theory of turbulence, recourse must be made to experimental results incorporated into suitable ad hoc theories.

Smoothing

The first step in any reduction of turbulent skin friction is to ensure that the surface is maintained smooth and constructed without any discontinuities and projections of any kind. A rough surface increases drag by increasing the local skin friction. Surface discontinuities and projections increase drag by producing local flow separations accompanied by pressure drag. The degree of surface smoothness does not have to equal that of machined surfaces in sliding contact. Quantitatively, this degree of hydrodynamic smoothness termed hydraulic smoothness, has been developed for Nikuradse-type sand grain roughness.[5] It is related to the thickness of the laminar sublayer. However, as yet there have been no comparable quantitative criteria developed for arbitrary irregular roughnesses such as found in practice.

Polymer Additives

Experimentally it has been found that small concentrations of long-chain polymers such as polyethylene oxide or polyacrylamide significantly reduce the turbulent skin friction.[24] The exact mechanism is not known but the experimental results have been correlated by extensions of the similarity laws for turbulent flow.[25] The main drawback in using polymers to reduce the drag of underwater bodies is the need for continually supplying polymer additives. The reduction of turbulent skin friction by polymer additives is a relatively reliable method because of its insensitivity to environmental conditions such as body roughness, unlike the drag-reduction methods dependent on stabilizing the laminar boundary layer.

Compliant Walls

There is experimental evidence that compliant walls may reduce turbulent skin friction under certain conditions.[26] The required elastic properties of the compliant material are still under investigation. There seems to be a complex interation of the vibrations of the compliant wall with the turbulence structure next to the wall. It is difficult in general to design a coating compliance to suit a wide range of flow conditions.

REFERENCES

1. Granville, P.S., "Geometrical Characteristics of Streamlined Shapes," Journal of Ship Research, Vol. 13, No. 4, pp. 299-313 (Dec 1969).

2. Granville, P.S., "Geometrical Characteristics of Flat-Faced Bodies of Revolution," Journal of Hydronautics, Vol. 7, No. 4, pp. 166-169 (Oct 1973).

3. Granville, P.S., "Geometrical Characteristics of Noses and Tails for Parallel Middle Bodies," International Shipbuilding Progress, Vol. 21, No. 233, pp. 3-19 (Jan 1974).

4. Smith, A.M.O. and J. Pierce, "Exact Solution of the Neumann Problem. Calculation of Non-Circulatory Plane and Axially Symmetric Flows About or Within Arbitrary Boundaries," Douglas Aircraft Co. Report ES-36988 (Apr 1958).

5. Granville, P.S., "Drag and Turbulent Boundary Layer of Flat Plates at Low Reynolds Numbers," David Taylor Naval Ship R&D Center Report 4682 (Dec 1975).

6. Gertler, M., "Resistance Experiments on a Systematic Series of Streamlined Bodies of Revolution for Application to the Design of High-Speed Submarines," David Taylor Model Basin Report C-297 (Apr 1950).

7. Eggers, H.A. and J.L. Beveridge, "The Mark 41 Torpedo Resistance and Propulsion Characteristics," David Taylor Model Basin Report C-400 (Feb 1951).

8. Eggers, H.A., "Torpedo Mark 43 MOD 0 - Resistance and Propulsion Characteristics," David Taylor Model Basin Report C-499 (Apr 1952).

9. Eggers, H.A., "Mark 41 Torpedo - Resistance and Propulsion Characteristics with Varying Body Lengths," David Taylor Model Basin Report C-526 (Sep 1952).

10. Larsen, C.A., "Additional Tests of Series 58 Forms - Part 1 - Resistance Tests of Parallel Middle Body Series," David Taylor Model Basin Report C-738 (Nov 1955).

11. Nelson, D.M., "Development of a Blunt Afterbody Configuration for the RETORC I Torpedo," Naval Undersea Warfare Center Report, NUWC TP 15 (Feb 1968).

12. Catz, J. and D. Paster, "Methods for Estimating Torpedo Power Requirements," U.S. Naval Underwater Ordnance Station (Newport, R.I.) Technical Memorandum 62 (Jul 1953).

13. Brooks, J.D. ad T.G. Lang, "Simplified Methods for Estimating Torpedo Drag," in "Underwater Propulsion," L. Greiner, ed., Compass Publications, Arlington, Va. (1967).

14. Granville, P.S., "The Calculation of the Viscous Drag of Bodies of Revolution," David Taylor Model Basin Report 849 (Jul 1953).

15. Granville, P.S., "Partial Form Factors from Equivalent Bodies of Revolution for the Froude Method of Predicting Ship Resistance," Society of Naval Architects and Marine Engineers, First Ship Technology and Research Symposium, Washington, D.C. (Aug 1975).

16. Carmichael, B.H., "Underwater Drag Reduction through Optimum Shape," in "Underwater Propulsion," L. Greiner, ed., Compass Publications, Arlington, Va. (1967).

17. Parsons, J.S., R.E. Goodson, and F.R. Goldschmied, "Shaping of Axisymmetric Bodies for Minimum Drag in Incompressible Flow," Journal of Hydronautics, Vol. 8, No. 3, pp. 100-107 (Jul 1974).

18. Granville, P.S., "The Prediction of Transition from Laminar to Turbulent Flow in Boundary Layers on Bodies of Revolution," Naval Ship R&D Center Report 3900 (Sep 1974).

19. Kaups, K., "Transition Prediction on Bodies of Revolution," Douglas Aircraft Co. Report MDC (Apr 1974).

20. Gregory, N., "Research on Suction Surfaces for Laminar Flow," in "Boundary Layer and Flow Control, Vol. 2," G.V. Lachmann, ed., Pergamon Press, London (1961).

21. Pfenninger, W. and J.W. Bacon, Jr., "About the Development of Swept Laminar Suction Wings with Full Chord Laminar Flow," in "Boundary Layer and Flow Control, Vol. 2," G.V. Lachmann, ed., Pergamon Press, London (1961).

22. Kramer, M.O., "Hydrodynamics of the Dolphin," in "Advances in Hydroscience, Vol. 2," V.T. Chow, ed., Academic Press, New York (1965).

23. Wazzan, A.R., T. Okamura, and A.M.O. Smith, "The Stability of Water Flow Over Heated and Cooled Flat Plates," Trans. ASME, Series C, Journal of Heat Transfer, Vol. 90, pp. 109-114 (Feb 1968).

24. Hoyt, J.W., "The Effect of Additives on Fluid Friction," Trans. ASME, Journal of Basic Engineering, Vol. 94, Series D, No. 2, pp. 258-285 (Jun 1972).

25. Granville, P.S., "Hydrodynamic Aspects of Drag Reduction with Additives," Marine Technology, Vol. 10, No. 3, pp. 284-292 (Jul 1973).

26. Fischer, M.C., L.M. Weinstein, R.L. Ash, and D.M. Bushnell, "Compliant Wall-Turbulent Skin-Friction Reduction Research," presented to 8th AIAA Fluid and Plasma Dynamics Conference, Hartford, Conn. (Jun 1975).

TABLE OF MASS DENSITY ρ OF WATER IN ENGLISH UNITS

(10th International Towing Tank Conference)

Fresh Water Mass Density $lb \cdot sec^2/ft^4$	Temperature ^oF	Sea Water Mass Density $lb \cdot sec^2/ft^4$	Fresh Water Mass Density $lb \cdot sec^2/ft^4$	Temperature ^oF	Sea Water Mass Density $lb \cdot sec^2/ft^4$
1.9399	32	1.9947	1.9383	60	1.9903
1.9399	33	1.9946	1.9381	61	1.9901
1.9400	34	1.9946	1.9379	62	1.9898
1.9400	35	1.9945	1.9377	63	1.9895
1.9401	36	1.9944	1.9375	64	1.9893
1.9401	37	1.9943	1.9373	65	1.9890
1.9401	38	1.9942	1.9371	66	1.9888
1.9401	39	1.9941	1.9369	67	1.9885
1.9401	40	1.9940	1.9367	68	1.9882
1.9401	41	1.9939	1.9365	69	1.9879
1.9401	42	1.9937	1.9362	70	1.9876
1.9401	43	1.9936	1.9360	71	1.9873
1.9400	44	1.9934	1.9358	72	1.9870
1.9400	45	1.9933	1.9355	73	1.9867
1.9399	46	1.9931	1.9352	74	1.9864
1.9398	47	1.9930	1.9350	75	1.9861
1.9398	48	1.9928	1.9347	76	1.9858
1.9397	49	1.9926	1.9344	77	1.9854
1.9396	50	1.9924	1.9342	78	1.9851
1.9395	51	1.9923	1.9339	79	1.9848
1.9394	52	1.9921	1.9336	80	1.9844
1.9393	53	1.9919	1.9333	81	1.9841
1.9392	54	1.9917	1.9330	82	1.9837
1.9390	55	1.9914	1.9327	83	1.9834
1.9389	56	1.9912	1.9324	84	1.9830
1.9387	57	1.9910	1.9321	85	1.9827
1.9386	58	1.9908	1.9317	86	1.9823
1.9384	59	1.9905			

TABLE OF MASS DENSITY ρ OF WATER IN METRIC UNITS

(10th International Towing Tank Conference)

Fresh Water Mass Density $kg \cdot sec^2/m^4$	Temperature ^oC	Sea Water Mass Density $kg \cdot sec^2/m^4$	Fresh Water Mass Density $kg \cdot sec^2/m^4$	Temperature ^oC	Sea Water Mass Density $kg \cdot sec^2/m^4$
101.95	0	104.83	101.86	16	104.59
101.95	1	104.82	101.84	17	104.56
101.96	2	104.81	101.82	18	104.54
101.96	3	104.81	101.80	19	104.52
101.96	4	104.80	101.78	20	104.49
101.96	5	104.79	101.76	21	104.46
101.96	6	104.77	101.74	22	104.43
101.95	7	104.76	101.71	23	104.40
101.95	8	104.74	101.69	24	104.37
101.94	9	104.73	101.66	25	104.34
101.93	10	104.71	101.64	26	104.31
101.92	11	104.69	101.61	27	104.28
101.91	12	104.68	101.58	28	104.24
101.90	13	104.65	101.55	29	104.21
101.88	14	104.63	101.52	30	104.18
101.87	15	104.61			

TABLE OF KINEMATIC VISCOSITY ν OF WATER IN ENGLISH UNITS

(10th International Towing Tank Conference)

Fresh Water $\nu \times 10^5$ ft^2/sec	Temperature ^oF	Sea Water $\nu \times 10^5$ ft^2/sec	Fresh Water $\nu \times 10^5$ ft^2/sec	Temperature ^oF	Sea Water $\nu \times 10^5$ ft^2/sec
1.9231	32	1.9681	1.2083	60	1.2615
1.8871	33	1.9328	1.1910	61	1.2443
1.8520	34	1.8974	1.1741	62	1.2275
1.8180	35	1.8637	1.1576	63	1.2112
1.7848	36	1.8309	1.1415	64	1.1951
1.7527	37	1.7991	1.1257	65	1.1794
1.7215	38	1.7682	1.1103	66	1.1638
1.6911	39	1.7382	1.0952	67	1.1489
1.6616	40	1.7091	1.0804	68	1.1342
1.6328	41	1.6807	1.0660	69	1.1198
1.6049	42	1.6532	1.0519	70	1.1057
1.5777	43	1.6263	1.0381	71	1.0918
1.5512	44	1.6002	1.0245	72	1.0783
1.5254	45	1.5748	1.0113	73	1.0650
1.5003	46	1.5501	0.9984	74	1.0520
1.4759	47	1.5259	0.9857	75	1.0392
1.4520	48	1.5024	0.9733	76	1.0267
1.4288	49	1.4796	0.9611	77	1.0145
1.4062	50	1.4572	0.9492	78	1.0025
1.3841	51	1.4354	0.9375	79	0.9907
1.3626	52	1.4142	0.9261	80	0.9792
1.3416	53	1.3935	0.9149	81	0.9678
1.3212	54	1.3732	0.9039	82	0.9567
1.3012	55	1.3536	0.8931	83	0.9457
1.2817	56	1.3343	0.8826	84	0.9350
1.2627	57	1.3154	0.8722	85	0.9245
1.2441	58	1.2970	0.8621	86	0.9142
1.2260	59	1.2791			

TABLE OF KINEMATIC VISCOSITY ν OF WATER IN METRIC UNITS

(10th International Towing Tank Conference)

Fresh Water $\nu \times 10^6$ m^2/sec	Temperature ^oC	Sea Water $\nu \times 10^6$ m^2/sec	Fresh Water $\nu \times 10^6$ m^2/sec	Temperature ^oC	Sea Water $\nu \times 10^6$ m^2/sec
1.7867	0	1.8264	1.1097	16	1.1592
1.7270	1	1.7692	1.0816	17	1.1312
1.6704	2	1.7131	1.0546	18	1.1044
1.6166	3	1.6599	1.0286	19	1.0785
1.5656	4	1.6094	1.0037	20	1.0537
1.5170	5	1.5614	0.9798	21	1.0298
1.4707	6	1.5158	0.9568	22	1.0068
1.4267	7	1.4724	0.9347	23	0.9846
1.3847	8	1.4310	0.9134	24	0.9632
1.3446	9	1.3915	0.8929	25	0.9425
1.3064	10	1.3538	0.8731	26	0.9226
1.2699	11	1.3177	0.8541	27	0.9033
1.2350	12	1.2832	0.8357	28	0.8847
1.2016	13	1.2503	0.8180	29	0.8667
1.1696	14	1.2186	0.8009	30	0.8493
1.1390	15	1.1888			

APPENDIX - ESTIMATION OF DRAG OF UNDERWATER BODIES

As an example of the details in evaluating the drag of a proposed underwater body, let us consider a body of length, L = 240 inches = 20 feet = 6.10 meters and of maximum diameter, D = 21 inches = 1.75 feet = 0.53 meter. which is to operate at a speed, U_∞ = 40 knots = 67.56 feet/sec = 20.59 meters/sec in sea water of temperature 58°F = 14.4°C.

To calculate the Reynolds number R_L, first find the kinematic viscosity ν of sea water at the temperature 58°F which from the table is $\nu = 1.2970 \times 10^{-5}$ feet^2/sec. The Reynolds number R_L is then

$$R_L = \frac{U_\infty L}{\nu} = \frac{(67.56)(20)}{1.2970 \times 10^{-5}} = 1.045 \times 10^8$$

The first step in obtaining drag coefficient C_D is to evaluate the flat-plate drag coefficient C_F from

$$C_F = \frac{0.0776}{(\log_{10} R_L - 1.88)^2} + \frac{60}{R_L} = \frac{0.0776}{[\log_{10}(1.045 \times 10^8) - 1.88]^2} + \frac{60}{1.045 \times 10^8} = 2.059 \times 10^{-3}$$

The next step is to estimate form drag coefficient C_r from Figure 2. Curve A which gives values of C_r for manufactured torpedoes with control surfaces is to be used. For a diameter-length ratio, d/L = 21 inches/240 inches = 0.0875, $C_r = 0.690 \times 10^{-3}$. This C_r includes appendage drag and drag due to normal torpedo roughness.

The drag coefficient C_D is then

$$C_D = C_F + C_r = 2.059 \times 10^{-3} + 0.690 \times 10^{-3} = 2.749 \times 10^{-3}$$

To obtain the drag D the density ρ is first obtained from the table for sea water of temperature 58°F or $\rho = 1.9908$ lb-sec^2/ft^4. If the exact shape is not known, the surface areas may be estimated from the surface coefficients C_s shown in Figure 1. For a diameter/length ratio of

0.0875, the curve for the Mark 41 torpedo gives a $C_s = 1.004$. The surface area S is then

$$S = C_s \pi d L = (1.004)\pi (1.75)(25) = 110.4 \text{ ft}^2 = 10.26 \text{ m}^2$$

The drag D is then

$$D = C_D \tfrac{1}{2} \rho U_\infty^2 S = \left(\frac{2.749 \times 10^{-3}}{2}\right)(1.9908)(67.56)^2(110.4) = 1379 \text{ lbs}$$
$$= 625.5 \text{ kgs}$$

The power is DU_∞ = (1380 lbs) (67.56 ft/sec) = 93,200 ft-lbs/sec = 170 horsepower.

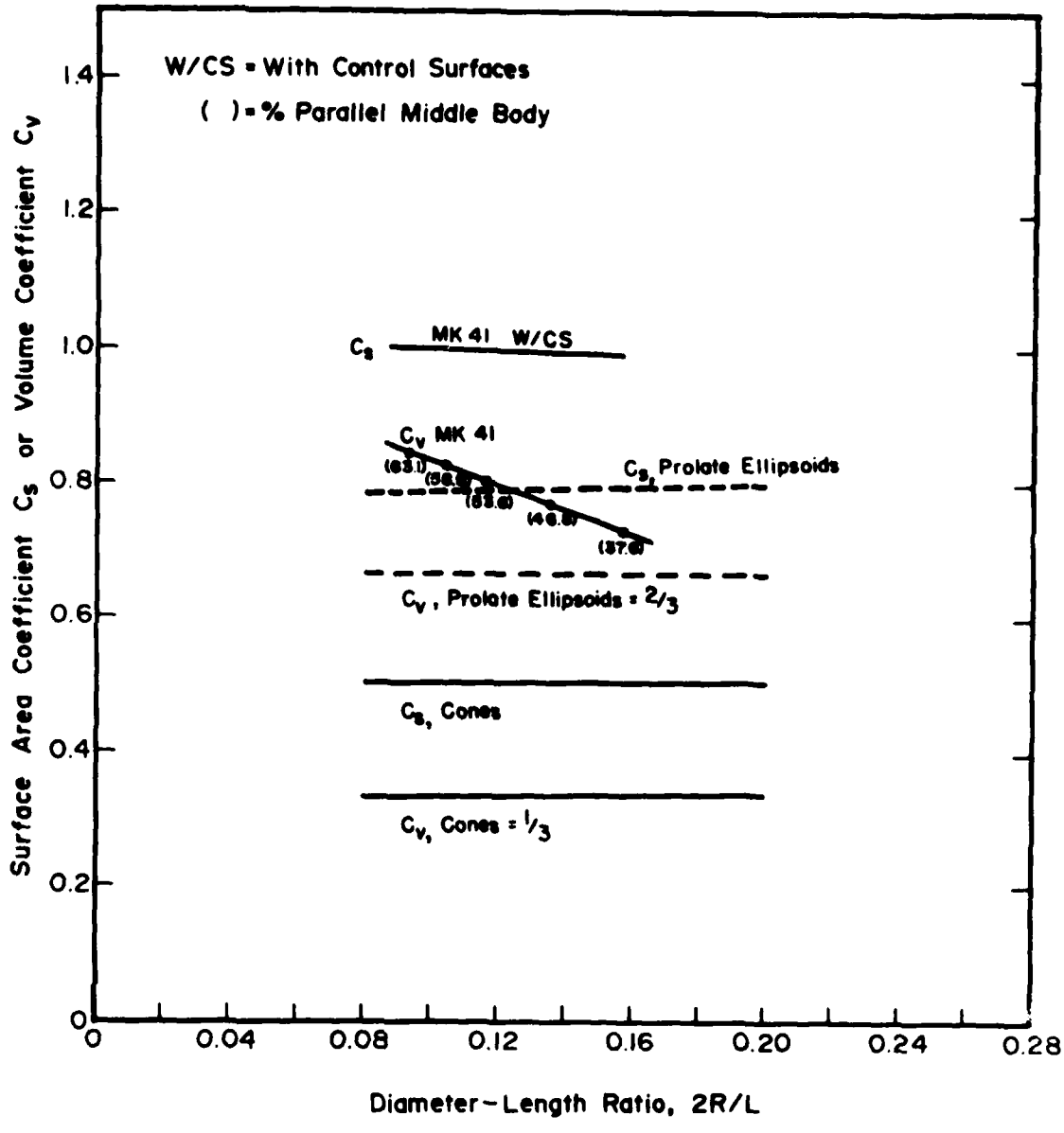

Figure 1 - Surface Area and Volume Coefficients

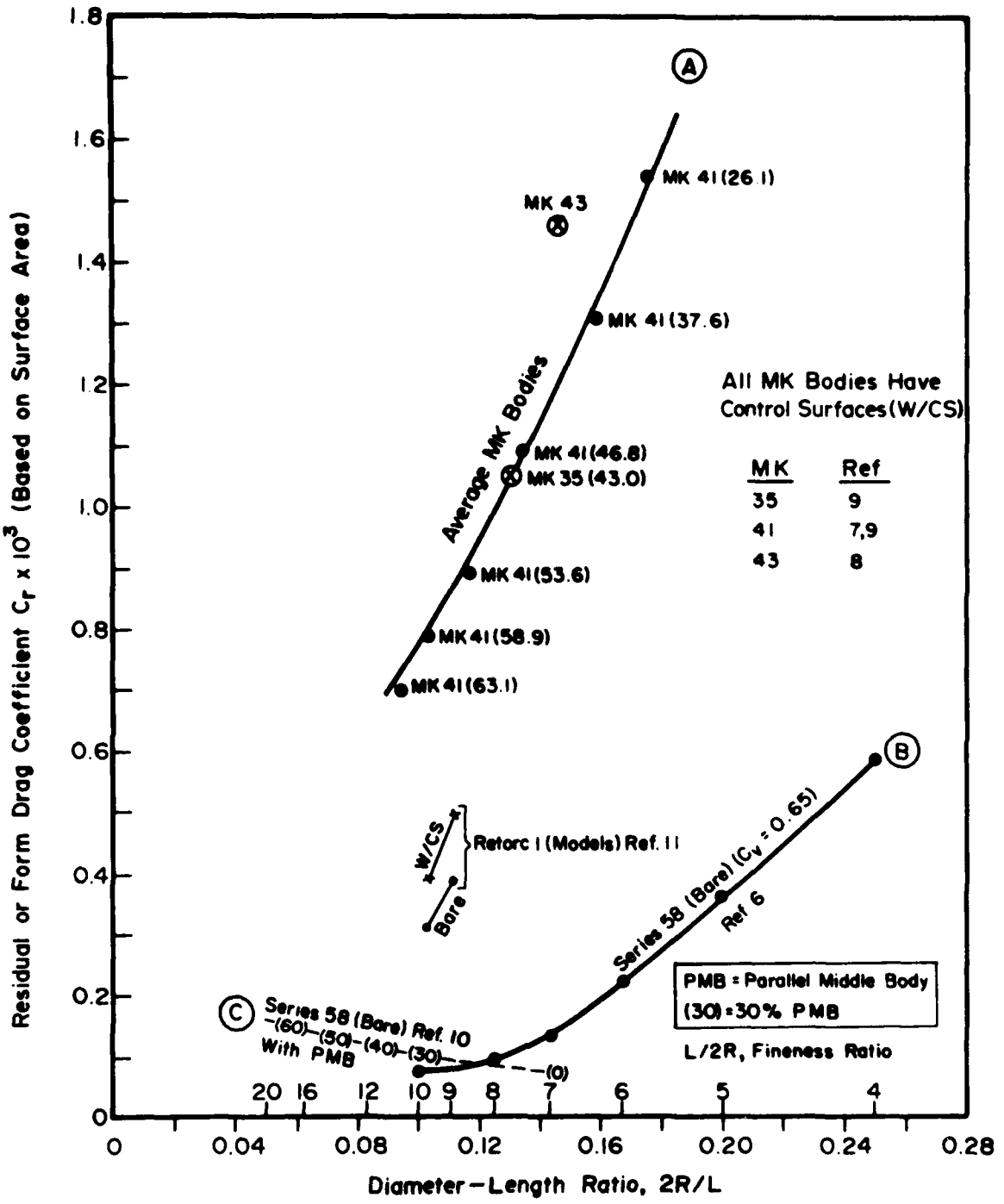

Figure 2–Form-Drag Coefficients for Various Bodies

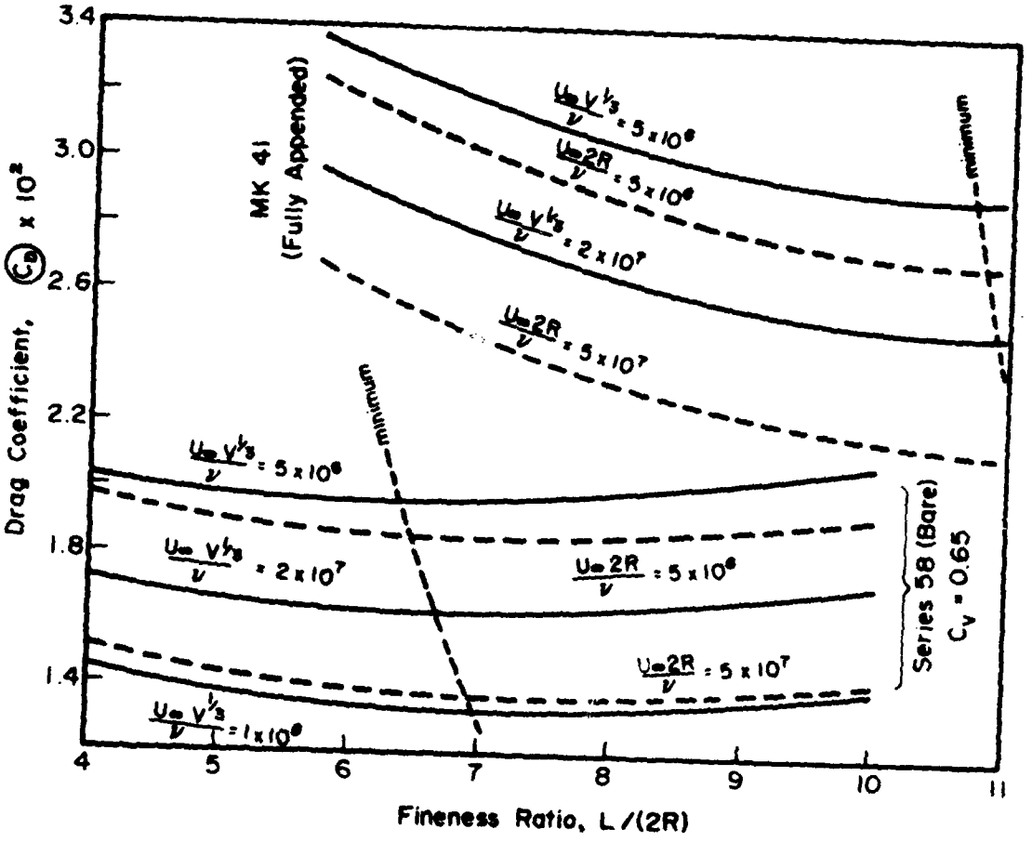

Figure 3 – Comparison of Drags of Bodies on a Volume Basis

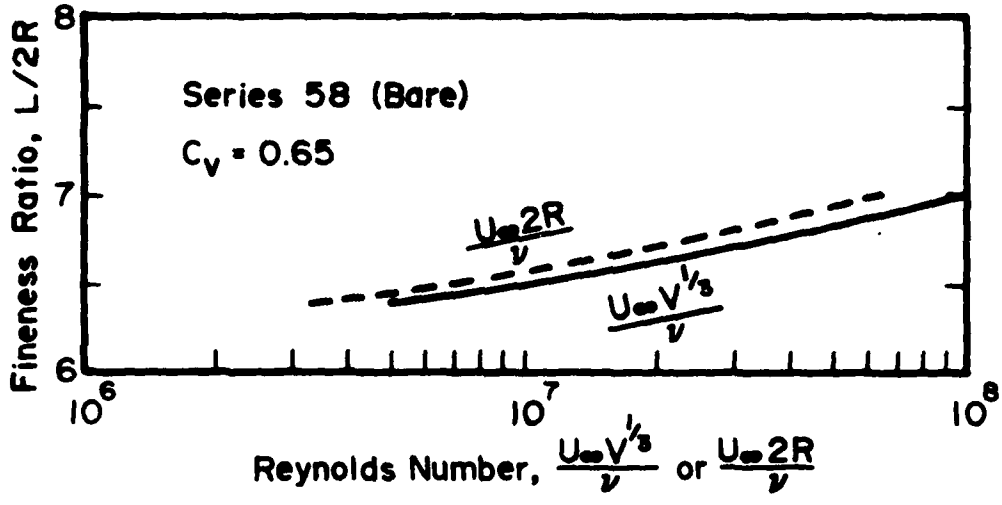

Figure 4 – Variation of Fineness Ratio with Reynolds Number for Minimum Drag Based on Volume

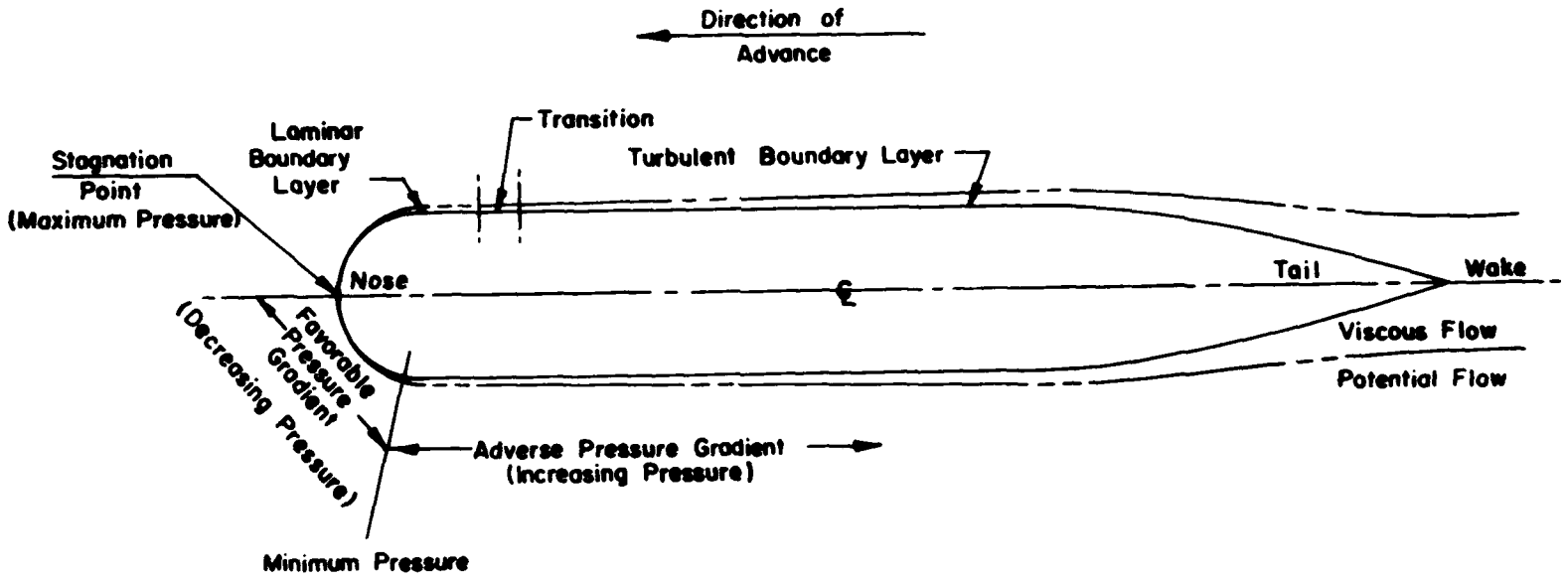

Figure 5 – Boundary Layer on a Body of Revolution

DTNSRDC ISSUES THREE TYPES OF REPORTS

(1) DTNSRDC REPORTS, A FORMAL SERIES PUBLISHING INFORMATION OF PERMANENT TECHNICAL VALUE, DESIGNATED BY A SERIAL REPORT NUMBER

(2) DEPARTMENTAL REPORTS, A SEMIFORMAL SERIES, RECORDING INFORMATION OF A PRELIMINARY OR TEMPORARY NATURE, OR OF LIMITED INTEREST OR SIGNIFICANCE, CARRYING A DEPARTMENTAL ALPHANUMERIC IDENTIFICATION.

(3) TECHNICAL MEMORANDA, AN INFORMAL SERIES, USUALLY INTERNAL WORKING PAPERS OR DIRECT REPORTS TO SPONSORS, NUMBERED AS TM SERIES REPORTS; NOT FOR GENERAL DISTRIBUTION.